



Energy research Centre of the Netherlands

# **Characteristics of the ultrafine particle fraction along motorways**

**Number concentrations, size distributions, emission factors and dynamical processes**

**E.P. Weijers**

**B. Verheggen**

**G.P.A. Kos**

**P.A.C. Jongejan**

## Acknowledgement

Part of the data collection and interpretation was done within the framework of the Netherlands Aerosol Program. This study was sponsored by the Ministry of Economic Affairs (project 7.2745) and the Ministry of Housing and Environment (project 7.0179). The authors would like to thank H. Bloemen (RIVM) and A. Khlystov (Duke University, USA) for their critical comments and suggestions.

## Abstract

Number concentration data of ultrafine particles (diameter less than 100 nm) were collected along two Dutch motorways. Measurements were performed with a scanning mobility particle sizer (SMPS; size range 13-284 nm) and a condensation particle counter (CPC) sequentially positioned at increasing distances downwind from the roadside and at one upwind location measuring the background air. It is found that the magnitude of the local wind speed substantially affects particle number levels due to dilution: a higher wind speed results in fewer particles in the air. After correction for this effect the decrease in particle number downwind of the motorway can be described rather well by exponentially decaying functions.

The total number of ultrafine particles at 10 m distance from the roadside is 5-8 times higher than upwind. Numbers fall to half this maximum after about 75 m. From this it can be concluded that people residing within a distance of approximately 200 m of a motorway experience (much) higher ambient levels of ultrafine particles than others.

Most of the particles measured downwind are smaller than 50 nm; this 'nanoparticle' mode is usually absent in the upwind registrations. Another mode observed in the downwind observations peaks between 50 and 70 nm, becoming more outspoken at larger diameters with increasing distance from the motorway. Modelling the dynamical aerosol processes on two days reveals that the changes in the size distribution are primarily explained by the effects of dilution and condensation. The effect of coagulation appears to be minor.

Emission factors for ultrafine particle numbers are estimated  $0.3 \cdot 10^{15}$  particles/km<sup>-1</sup> for light-duty vehicles and  $3.1 \cdot 10^{15}$  particles/km<sup>-1</sup> for heavy-duty vehicles, which is in agreement with other findings reported in literature.

## Keywords

Particulate matter, ultrafine particles, number, size distribution, motorway, vehicle emissions, SMPS, CPC

# Contents

List of tables	4
List of figures	4
1. Introduction	7
2. Experimental techniques and methods	9
2.1 Sampling locations	9
2.2 Instrumentation	9
2.3 Determination of emission factors of ultrafine particles	10
3. Results and discussion	12
3.1 Wind effects	12
3.2 Traffic effects	15
3.3 Gradients of particle number concentrations	17
3.4 Changes in number size distributions at increasing distance from the motorway	18
3.5 Modelling aerosol dynamical processes	22
3.6 Emission factors for ultrafine particle number	27
4. Conclusions	30
References	32

## List of tables

Table 2.1	<i>Measurement days and instrumental set-up</i> .....	10
Table 3.1	<i>Estimated emission factors for ultrafine particle number (in number of particles per km and per vehicle)</i> .....	28

## List of figures

Figure 2.1	<i>The locations of the measurement sites near the A1- and A9-motorways (1 cm <math>\approx</math> 10 km)</i> .....	9
Figure 3.1	<i>One-minute measurements of normalized particle numbers (measured by CPC) and the deviation of the wind direction (<math>dd</math>) with the normal of the motorway orientation (<math>260^\circ</math>)</i> .....	12
Figure 3.2	<i>One-minute measurements of the particle numbers (measured by CPC) and local wind speed</i> .....	13
Figure 3.3	<i>One-minute measurements of the particle numbers measured by LAS-X and local wind speed</i> .....	13
Figure 3.4	<i>Average numbers of ultrafine particles (UF) measured upwind and at three distances downwind along the A1-motorway versus average local wind speed (<math>U</math>). Bars indicate one standard deviation</i> .....	14
Figure 3.5	<i>As Figure 3.4 but now for A9 data</i> .....	14
Figure 3.6	<i>Number of ultrafine particles (periods 1-4) and vehicular intensity (periods 2 and 3) measured along the A1 motorway. Period 1: upwind registration; period 2: ongoing traffic, vehicle speed around 90-100 km/h; period 3: continuous traffic flow, vehicle speed around 40 km/h; stagnant traffic conditions</i> .....	15
Figure 3.7	<i>Number distributions with corresponding standard deviation for period 2 and 3 (see Figure 3.6) with high (90-100 km/h) and low (40 km/h) vehicle propagation. Also given is the upwind size distribution (background)</i> . ....	16
Figure 3.8	<i>Gradients of the number of ultrafine particles (with standard deviation) along the A1 and A9 motorway (after correcting for the wind speed effect). Also given the average background concentration level and exponential approximations</i> ....	17
Figure 3.9	<i>Average particle size distributions for the 8 measurement days (corrected for wind speed dilution effect) at 10 m; measurement range SMPS-CPC: 13-284 nm diameter</i> . ....	18
Figure 3.10	<i>As Figure 3.9 but now at 45 m</i> .....	19
Figure 3.11	<i>As Figure 3.9 but now at 90 m</i> .....	19
Figure 3.12	<i>As Figure 3.9 but now at the upwind location</i> .....	20
Figure 3.13	<i>Average size distributions measured at 10, 45 and 90 m with upwind contribution subtracted</i> .....	21
Figure 3.14	<i>Relative decrease of particle numbers for three size fractions during the wind-driven transport from the 10 m site to the 90 m site</i> .....	22
Figure 3.15	<i>Measured size distributions (particles <math>\text{cm}^{-3}</math>) on September 26 (left panel), averaged for each distance to the motorway. The index number refers to the location, where <math>n_0</math> denotes 10 m downwind, <math>n_1</math> the 25 m, <math>n_2</math> the 40 m, and <math>n_3</math> the 80 m, and <math>n_4</math> is upwind of the motorway (background). The right panel gives the same distributions, corrected for dilution using <math>\text{NO}_x</math> as a tracer. Note that particle radius is used here instead of diameter</i> .....	22
Figure 3.16	<i>Decay of particle and <math>\text{NO}_x</math> concentrations with increasing travelling time (in seconds) from the motorway. The background values are arbitrarily set at 200 seconds. Particle concentrations (as measured by CPC and the SMPS integral,</i>	

	<i>N<sub>total</sub></i> are noted on the left axis (particles/cm <sup>3</sup> ) and NO <sub>x</sub> on the right axis (ppm). An exponential decay is fitted to the CPC and NO <sub>x</sub> data. ....	23
Figure 3.17	Radius growth rates as found using PARGAN by analysing the change in the dilution-corrected size distributions. ....	25
Figure 3.18	The contribution of different processes to the change in cumulative particle number size distribution (particles cm <sup>-3</sup> ). ....	25
Figure 3.19	The contribution of different processes to the change in particle number size distribution (particles cm <sup>-3</sup> ). ....	26
Figure 3.20	Growth rate and dilution rate constant, as found by regression analysis of the distributions measured on November 11. ....	26
Figure 3.21	The contribution of different processes to the change in cumulative particle number (particles cm <sup>-3</sup> ). The sum of condensation (=growth), coagulation and dilution gives the calculated change in cumulative number (black squares), which is as close as possible to the measured change (thick black line), by optimizing both the growth rate and the dilution rate (Figure 3.20). ....	27
Figure 3.22	Regression analyses for the A9 data. ....	29



## 1. Introduction

Over the last decades a large number of epidemiological studies have reported convincing relationships between the exposure to particulate matter and effects like premature mortality, morbidity and hospital admissions (e.g. Dockery et al., 1993; Künzli et al., 2000; Hoek et al., 2002). However, the debate on the pathogenetic mechanism still continues (e.g. Osunsanya et al., 2001). There are several hypotheses. One of them is that the large numbers of ultrafine particles (<100 nm diameter; UFP) measured in urban air cause the adverse effects. The UFP fraction dominates the urban aerosol numbers up to 80% (Morawska et al., 1998). It consists of a mixture of soot, acid condensates, sulphates and nitrates as well as trace metals. Medical research revealed that they penetrate deeply into the lungs (Jaques and Kim, 2000). Others (Peters et al., 1997) discovered that increased UFP levels tend to negatively influence the respiratory system of asthmatics. Various toxicological studies indicate that they do more harm to human health than larger particles with similar chemical composition and mass concentrations (Ferin et al., 1992; Donaldson, 1998; 2001).

In the European Union an air quality standard exists limiting the mass concentration of  $PM_{10}$  (<10  $\mu m$ ) and  $PM_{2.5}$  (CAFE, 2003). The ultrafines 'escape' these standards because they contribute very little to the total mass of particulate matter in air. In the measurements the presence of these very fine particles is easily obscured by only a few larger particles. The study of the 'ultrafines' and their possible health effects also demands a different experimental approach. Many researchers measured elevated particle number concentrations in an urban environment (e.g. Weijers et al., 2004; Pirjola et al., 2004). Motor vehicle emissions are known to contribute largely to their presence. Size measurements directly on diesel exhaust showed that most of the ultrafines are submicrometer agglomerates of carbonaceous particles ranging from 20 to 120 nm. On-road measurements revealed that the majority of these particles has a aerodynamic diameter that is less than 50 nm (Kittelson, 2004). Size distributions from gasoline vehicles tend to smaller mean diameters, i.e. 40-80 nm (Ristovski et al., 1998; Harris and Maricq, 2001). More experimental data on UFP are needed to quantify the particle number emission factors and the distance near roads over which ultrafines still contribute significantly on top of background levels. Also, such data are necessary to investigate their behaviour during the wind-driven transport under the influence of atmospheric dilution, condensation deposition, and coagulation. More insight in these topics is of particular interest for an improved quantification of the exposure of humans residing in the vicinity of busy traffic.

In Australia Morawska et al. (1999) measured the horizontal profiles of submicrometer particulates at two selected sites in the urban area of Brisbane, Australia. There was no significant decrease in particle number concentration with distance from the road for the first site but there was a decrease in concentration at the second site. This difference is believed to be due to the topography of the sites and it was concluded that further studies should take place at less disturbed sites. Hitchins et al. (2000; also in Australia) investigated size distributions (15 nm to 20  $\mu m$ ) and number concentrations at distances from the road ranging from 15 and 375 m. They discovered that when the wind is blowing directly from the road, concentration at a 100-150 m distance decayed to around half the values measured at 15 m. Shi et al. (1999; 2001) observed a faster decline of particle number concentration than of mass concentration and concluded that dilution with background air is the main dynamical mechanism influencing number concentrations. Zhu (2002a; 2002b) observed that the ultrafine particle concentrations at 300 m downwind from a motorway became indistinguishable from the upwind (background) levels This study further revealed that both dilution and coagulation play an important role in the change in particle size distribution with distance from a motorway.

Despite considerable improvements during the last three decades the Netherlands continue to exhibit a severe particulate air quality problem. Although new technologies and improved fuel composition decreases the particulate matter emitted by vehicles, problems still remain at a number of places in urban areas. Motivated by the growing concern on health and the need to quantify the human exposure to UFP for epidemiological studies, a measurement campaign was initiated within the framework of the Netherlands Aerosol Programme (Buringh and Opperhuizen, 2002) leading to the first dataset in the Netherlands with respect to the ‘vehicular induced’ ultrafine fraction. The study here typically focuses on changes in particle number concentrations and size distributions with increasing distance from the motorway and discusses the major particle dynamical mechanisms inducing these changes. In addition, the acquired dataset made it possible to estimate emission factors for the UFP fraction along the motorways.



## 2. Experimental techniques and methods

### 2.1 Sampling locations

The measurements were performed along two motorways (A1 and A9) located in non-urbanized areas in the province of Noord-Holland (Figure 2.1). The main criteria for both sites were that the vicinity should be relatively flat, that no other significant local sources of particulate matter should be present, and that high traffic densities can be expected. The selected experimental sites were located south of the A1-motorway between Amsterdam and Muiden (east of Amsterdam), and east of the A9-motorway between Amsterdam and Alkmaar (northwest of Amsterdam; see Figure 2.1). The A1-motorway is an 8-lane asphalt road (including two side lanes and 4 m grass area between the directions), it runs generally west and east (actual orientation 260°). The upwind terrain is predominantly flat-mowed lawn for 1.5 km with a row of mature trees about 100 m north of the motorway. Apart from the trees there are no further obstacles upwind. South of the motorway there are flat meadowlands. The A9 runs practically north to south (350°). The surrounding terrain is flat meadowland with only a few scattered storage buildings not higher than 3 m. The meadowlands extend 2 km to the east and west of the motorway and for 1.5 km along the motorway. Measurements were done here made on a small labour road with brick stones and hardly any traffic. At the site of the measurements the A9 has 6 lanes, (including two hard-shoulder side lanes). No other motorways or major roads are nearby. The location of each downwind measurement site was determined by measuring its distance from the roadside. The vehicles contribution is studied here by considering the upwind-downwind differences.

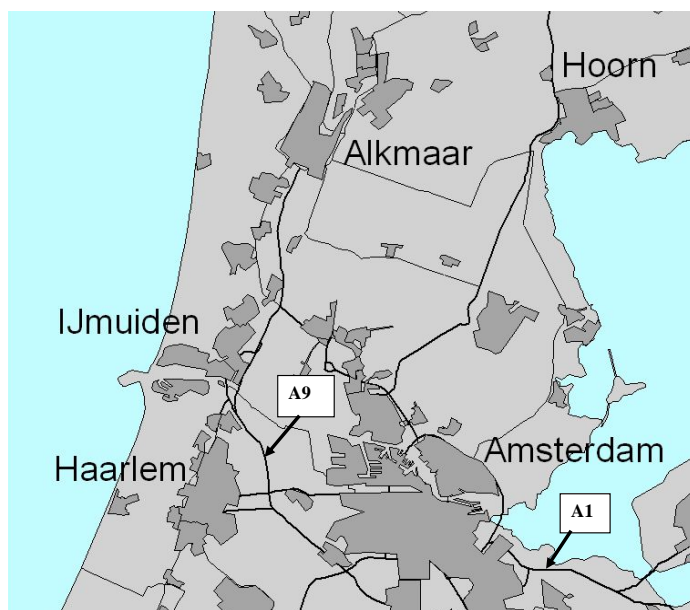


Figure 2.1 *The locations of the measurement sites near the A1- and A9-motorways (1 cm  $\approx$  10 km)*

### 2.2 Instrumentation

A mobile laboratory provided measurements of particles, some gaseous pollutants, meteorological and geographical parameters. A Scanning Mobility Particle Sizer (SMPS, TSI Inc.) measured the number distribution in the size range 13-284 nm. The instrument consists of an electrostatic classifier (EC) and a condensation particle counter (CPC3022, TSI Inc.). It uses

the bipolar charger in the EC to charge particles to a known distribution. The particles are then classified according to their ability to traverse an electrical field and counted by the CPC. The operation of the SMPS system involves choices of sheath airflow rates that determine the measurable size range. The flow rate was adjusted to 1 l/min in order to minimise diffusion losses. All tubing consisted of copper metal with a length of about 1.5 m and a 1/4-inch diameter. Diffusion losses in the tube were taken into account when analysing the data by use of a special correction scheme (Hinds, 1982). A dryer was inserted for maintaining a constant humidity. The sizing accuracy of the SMPS was verified in the laboratory with monodisperse polystyrene latex spheres (PSL, Polysciences Inc.). Scan time per sample was 2.5 min and data were stored on a PC. Additionally, the total number concentration of particles larger than 3 nm was detected by a CPC 3025 (TSI Inc) and also LAS-X measurements were incidentally executed for the size range 0.1-7.5 µm.

The measurements presented herein were conducted on eight weekdays in the period September-November 2002. The downwind sites were at 10, 45 and 90 m measured from the curb of the motorway. Background concentrations were determined upwind some 300 m from the roadside. Table 2.1 provides the measurement days and summarizes the instruments that were used on each day. One sampling period lasted 15-30 min. As soon as the sampling finished, the van was driven to the next site where measurements started again. It took about three hours to complete a set of four distances including the measurement at the background site. Two or three sets could be performed on each sampling day. The occurrence of traffic jams or limited traffic flow was monitored visually.

Concentrations of carbon monoxide (CO), nitrogen monoxide (NO) as well as nitrogen oxides (NO<sub>x</sub>) were monitored simultaneously at each sampling site along the A9. The acquired data were later averaged over the time periods corresponding to the SMPS scanning intervals. During the measurements wind direction and wind speed were measured at about 3 m above ground level. These data were averaged over one-minute intervals and logged into a computerised weather station.

Table 2.1 *Measurement days and instrumental set-up*

<i>Date</i>	<i>Motorway</i>	<i>CPC-3022</i>	<i>SMPS</i>	<i>CPC-3025</i>	<i>Las-X</i>	<i>NOx</i>	<i>CO</i>	<i>meteorology</i>
<i>19-sep-02</i>	A1	x	x					x
<i>20-sep-02</i>	A1	x	x					x
<i>23-sep-02</i>	A1	x	x					x
<i>25-sep-02</i>	A1	x	x					x
<i>26-sep-02</i>	A9	x	x			x	x	x
<i>07-nov-02</i>	A9	x	x			x	x	x
<i>11-nov-02</i>	A9	x	x	x	x	x	x	x
<i>12-nov-02</i>	A9	x	x	x	x	x	x	x

### 2.3 Determination of emission factors of ultrafine particles

Emission factors for the ultrafine particle fraction were determined according to the ‘open-air’ method of Bloemen and van Putten (1998). A concise description of their approach follows here. It is assumed that the contribution due to the traffic ( $C_t$ ) is given by the difference of a measured concentration ( $C_{meas}$ ) of some pollutant downwind from the road and its background level ( $C_{bg}$ ) measured upwind:

$$C_t = C_{meas} - C_{bg}. \quad [1]$$

The vehicular contribution can also be written as

$$C_t = N E_f f_{\text{disp}}, \quad [2]$$

where  $N$  is the number representing the traffic intensity,  $E_f$  the emission factor and  $f_{\text{disp}}$  the dispersion factor. Light- and heavy-duty vehicles (LDV and HDV) emit pollutants in different amounts and composition. It is possible to distinguish between both types of vehicles:

$$C_t = N [f_h E_h + (1 - f_h) E_l] f_{\text{disp}}, \quad [3]$$

with  $f_h$  the fraction of HDV on the motorway, and  $E_h$  and  $E_l$  the emission factors of HDV and LDV, respectively. Eliminating the unknown  $f_{\text{disp}}$ ,  $N$  and  $f_h$  by applying Eq.[3] to the vehicular contributions  $\text{PM}_t$ ,  $\text{CO}_t$  and  $\text{NO}_{xt}$  ultimately yields (after some mathematical manipulation) the following linear equation:

$$\text{PM}_t / \text{CO}_t = p + q \text{NO}_{xt} / \text{CO}_t. \quad [4]$$

Parameters  $p$  and  $q$  can be determined by least-square regression on the concentrations of  $\text{PM}_t$ ,  $\text{NO}_{xt}$  and  $\text{CO}_t$  that are measured near the road (motorway). The PM emission factors for traffic are then extracted as:

$$E_h^{\text{PM}_t} = p E_h^{\text{CO}_t} + q E_h^{\text{NO}_{xt}} \text{ and } E_l^{\text{PM}_t} = p E_l^{\text{CO}_t} + q E_l^{\text{NO}_{xt}}. \quad [5]$$

It is now assumed that the dispersion of particles in air is the same as that of gasses (which is true for particles with diameters less than 1  $\mu\text{m}$  and for the short distances between generation of the particles and inlet of the measuring system). The expression for the number of (ultrafine) particles ( $n$ ) due to HDV and LDV emissions can then be obtained similarly:

$$E_h^{n \text{UF}_t} = p' E_h^{\text{CO}_t} + q' E_h^{\text{NO}_{xt}} \text{ and } E_l^{n \text{UF}_t} = p' E_l^{\text{CO}_t} + q' E_l^{\text{NO}_{xt}}. \quad [6]$$

Eqs.[6] provide the possibility of estimating vehicular emissions factors for (ultrafine) particle numbers by use of the simultaneously recorded vehicular contributions to number,  $\text{NO}_{xt}$  and  $\text{CO}_t$ , and the vehicular emission factors for CO and  $\text{NO}_x$  on a traffic road.

### 3. Results and discussion

#### 3.1 Wind effects

The direction of the prevailing wind vector (with respect to the orientation of the motorway) influences the particle number concentrations measured downwind. For example, Hitchins et al. (2000) showed different horizontal gradients of particle number depending on whether the wind was blowing directly from or parallel to the road. To circumvent such an effect data were used here when the wind direction was within a  $25^\circ$  arc of the normal to the orientation of the motorway. This is motivated by a comparison between one-minute data of wind direction and corresponding CPC number (A9 motorway, 11 and 12 November, 6 sampling periods, 104 data points). Distance of the site to the road is 45 m. Figure 3.1 shows these data as function of the difference between the normal to the motorway ( $260^\circ$ ) and the direction of the wind ( $dd$ ). Particle numbers were normalised by their corresponding sampling-period average. A (slight) tendency for numbers to decrease is seen when the deviation angle becomes larger. However, the effect appears to be minor for the wind sector considered ( $\pm 25^\circ$ ).

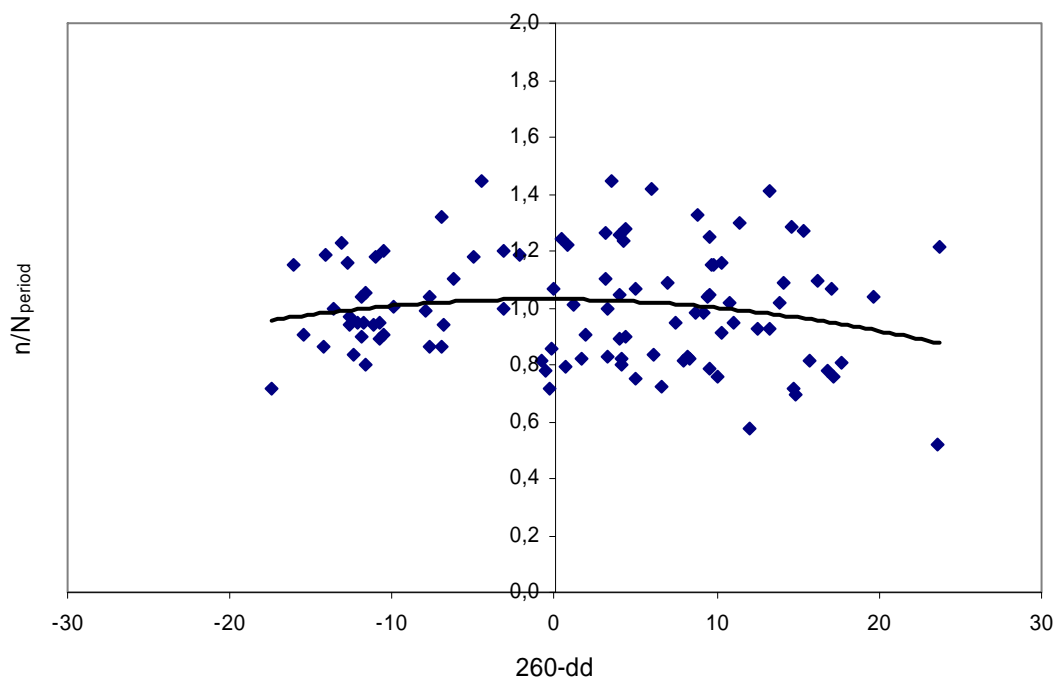


Figure 3.1 *One-minute measurements of normalized particle numbers (measured by CPC) and the deviation of the wind direction ( $dd$ ) with the normal of the motorway orientation ( $260^\circ$ )*

With the same dataset the effect of the local wind speed on total particle number was studied. The result is given in Figure 3.2. Although not statistically significant, a fitting procedure suggests an exponential decrease between total number and wind speed reflecting the idea that particle number is dominated by the ultrafine fraction which becomes more diluted in case of an increasing wind speed. The fraction of fine particles being (much) larger in diameter is predominantly affected by suspension and resuspension processes (Harrison et al., 2001, Charron and Harrison, 2003, Hussein et al., 2006). Indeed, looking at the LAS-X numbers (measuring particles with diameters between 0.1 and  $7.5 \mu\text{m}$ ) for the same periods (Figure 3.3) the shape is obviously different. Here, a rather minor increase with wind speed is observed.

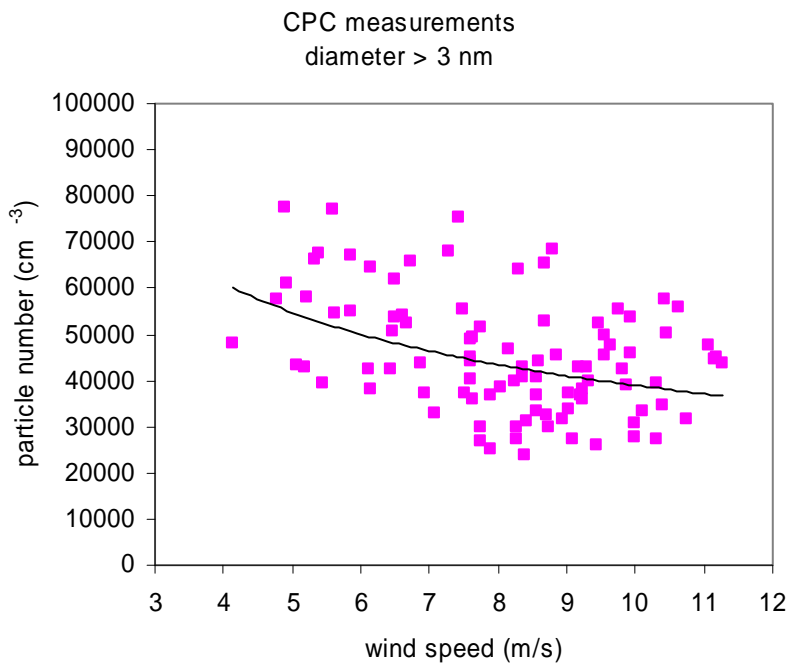


Figure 3.2 *One-minute measurements of the particle numbers (measured by CPC) and local wind speed*

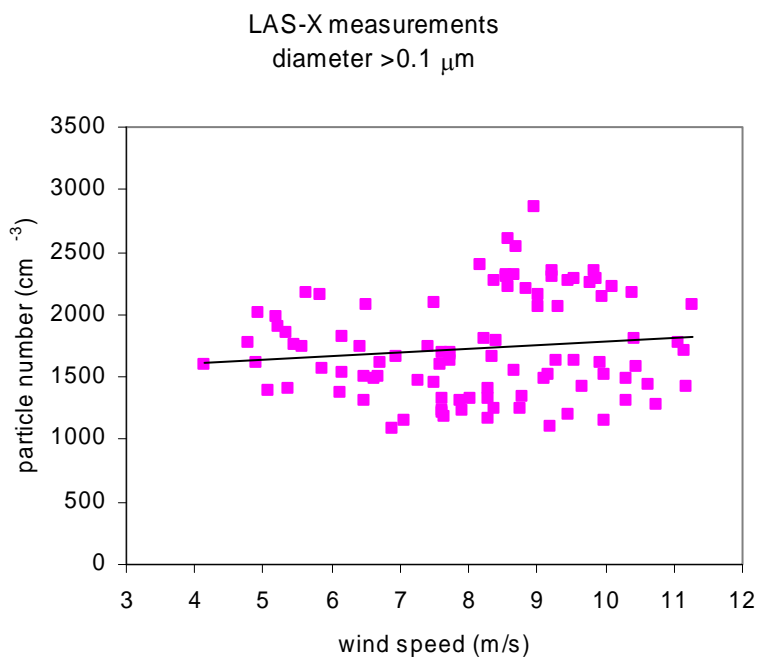


Figure 3.3 *One-minute measurements of the particle numbers measured by LAS-X and local wind speed*

Clearly, the effect of wind speed on particle number and distribution can be considerable. The average relationship between the numbers of ultrafine particles and wind speed was further investigated in Figure 3.4 and Figure 3.5 (measurements along the A1 and the A9). In these figures daily average ultrafine particle numbers measured at a 10, 45 and 90 m distance from the roadside are shown as function of the average local wind speed. The average background level

(measured upwind) has been subtracted. The dataset along the A9 suffers from a rather small range in the prevailing wind speeds. However, along the A1 the correspondence is in good approximation linear for the considered range in wind speed (3-8 m/s). It is concluded that in the study of average particle gradients and size distributions as a function of the downwind distance one needs to incorporate the effect of a varying atmospheric dilution due to the wind speed. These results are used in the assessment of number gradients and changes in number size distribution.

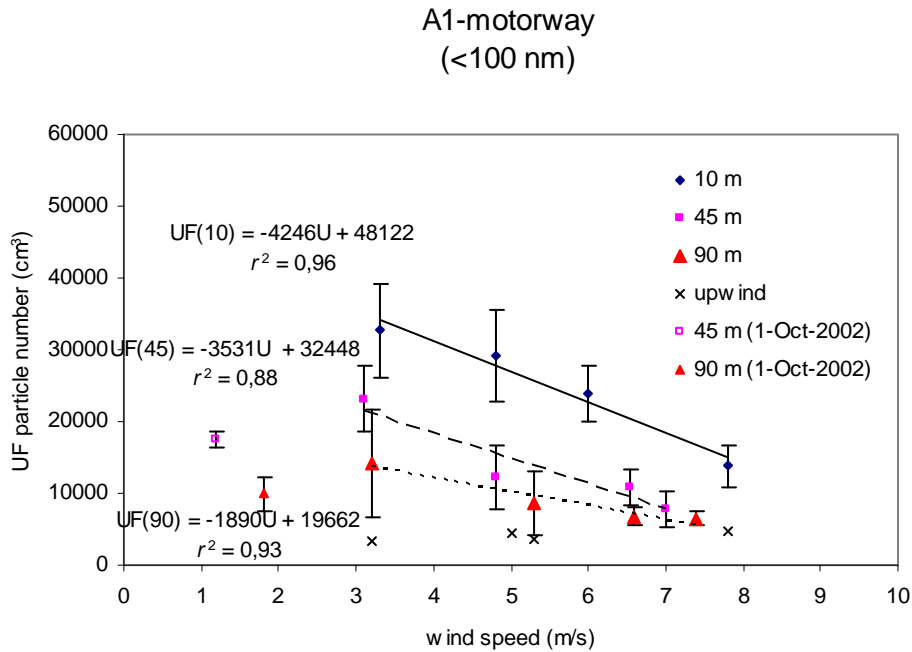


Figure 3.4 *Average numbers of ultrafine particles (UF) measured upwind and at three distances downwind along the A1-motorway versus average local wind speed (U). Bars indicate one standard deviation*

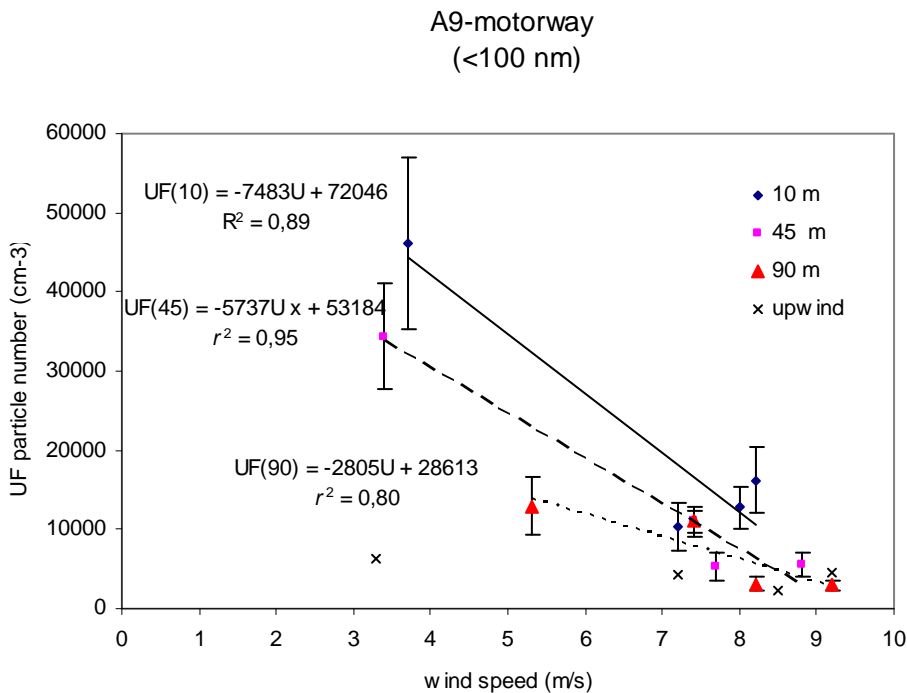


Figure 3.5 *As Figure 3.4 but now for A9 data*

Figure 3.4 also includes some data when wind speed was less than 2 m/s (A1, 1 October 2002). At this day a tendency for lower particle numbers is observed. For example, at 45 m from the motorway an average number of some  $17,500 \text{ cm}^{-3}$  is measured during a period with an average wind speed of 1.2 m/s. A second example, later that day, shows an average of  $9,800 \text{ cm}^{-3}$  and a wind speed of 1.8 m/s observed at 90 m. In both examples particle number is lower than the levels measured when the wind speed is around 3 m/s. This phenomenon has been observed earlier by Zhu et al. (2002). A possible explanation is that during low wind-speed conditions the travel of particles from the roadway to the measuring site will take more time and (ultrafine) particles have a larger chance to coagulate with other particles yielding a decrease in numbers.

### 3.2 Traffic effects

Online registrations were studied to characterize the near-road aerosol under various traffic conditions. Figure 3.6 shows the SMPS-integrated particle numbers and vehicular intensity during three different periods on one day (25 September). The first period shown contains the upwind registration with an average number concentration of around  $4300 \text{ cm}^{-3}$ . The remaining periods were measured at 10 m downwind from the roadside. The second period (15:00-15:50) reflects the common situation: ongoing traffic at a speed of around 90-100 km/h and 150 and 200 vehicles per minute. Particle numbers typically range from  $20,000\text{-}40,000 \text{ cm}^{-3}$ . This is 5 to 9 times higher than ultrafine number concentrations observed in upwind air indicating that vehicle emissions are the main contributor to the presence of ultrafine particles. Similarities can be recognized between the time series.

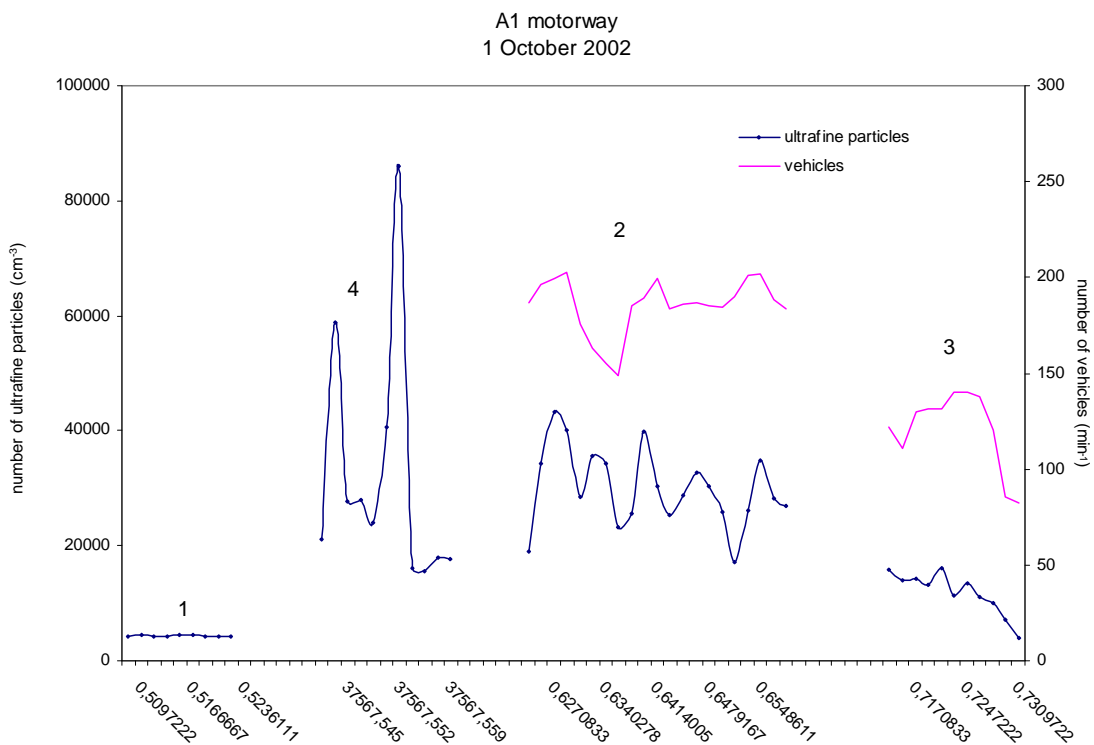


Figure 3.6 *Number of ultrafine particles (periods 1-4) and vehicular intensity (periods 2 and 3) measured along the A1 motorway. Period 1: upwind registration; period 2: ongoing traffic, vehicle speed around 90-100 km/h; period 3: continuous traffic flow, vehicle speed around 40 km/h; stagnant traffic conditions*

A traffic slowdown developed later that day (17:00-17:30). Propagation speed decreased with fewer vehicles passing by: some 110 per minute. The flow was still continuous but the estimated

vehicle speed came barely above 40 km/h. Ultrafine particle numbers decreased accordingly now being around  $15,000 \text{ cm}^{-3}$ . A lower vehicle speed is expected to influence the number of emitted particles in two ways: first, the motor system operates at a lower power producing less particles and lower mass concentrations. Second, when driving slowly the particles in the motor system have longer residence times. Coagulation rapidly decreases their output number (leaving total mass unchanged) in the case that the exhaust is not diluted rapidly (Kittelson, 1998; 2004).

However, even at lower speeds higher particle emissions occur as can be seen during the fourth period (13:00-13:30) when heavy congestion took place. Now, average and variability are strongly enhanced (maximum level above  $80,000 \text{ cm}^{-3}$ ). Similar findings have been observed during on-road measurements within so-called 'stop-and-go' traffic flows (Weijers et al., 2004). Here, the increase in particle numbers is probably due to the combination of an irregular load of the motor system (alternation of acceleration and deceleration) and more vehicles per kilometre road.

Varying vehicle speeds also affect the particle size distributions measured downwind which is demonstrated in Figure 3.7. Here, number distributions with corresponding standard deviations are given for periods 2 and 3, and for the background registration. Compared to background air, numbers and variability within the diameter range below 50 nm have increased considerably downwind of the motorway with higher numbers occurring at the higher vehicle propagation. In the further analysis on number gradients and size distributions stagnant traffic conditions have been discarded to ensure that the dataset is representative for a continuous traffic flow.

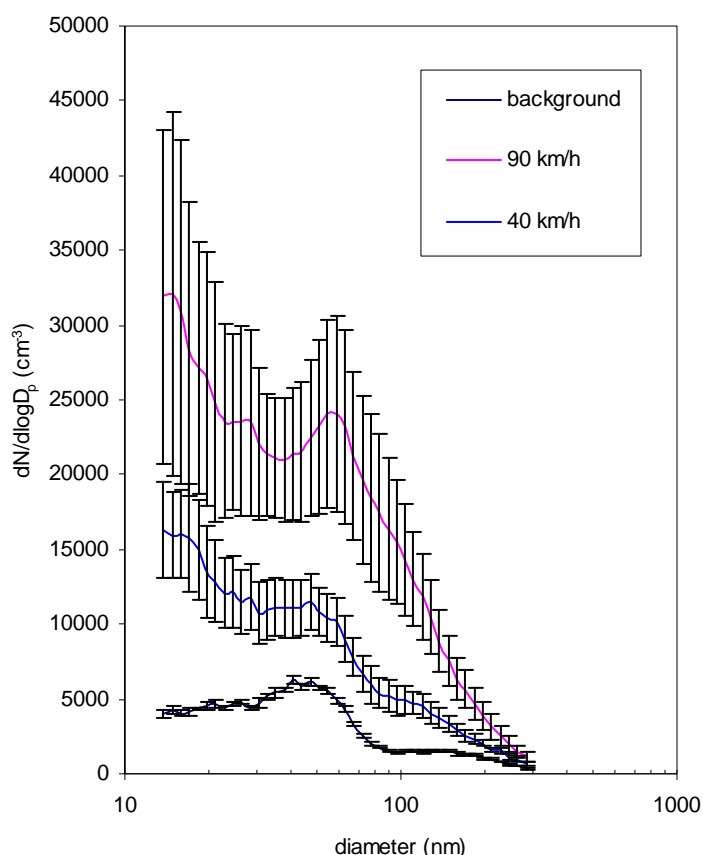


Figure 3.7 *Number distributions with corresponding standard deviation for period 2 and 3 (see Figure 3.6) with high (90-100 km/h) and low (40 km/h) vehicle propagation. Also given is the upwind size distribution (background).*



### 3.3 Gradients of particle number concentrations

Figure 3.4 and Figure 3.5 demonstrated the effect of the local wind speed on the number concentrations near the A1- and A9-motorway. In order to use the experimental results collected during subsequent periods the SMPS-CPC data were first normalised. This is done with the linear equations given in Figure 3.4 and Figure 3.5. As an example, the normalising equation for the data collected at 10 m from the A1-roadside reads as:

$$N_{UF}^n(10) = N_{UF}(10) \left( \frac{22464}{48122 - 4246U} \right). \quad (3.1)$$

Here,  $N_{UF}(10)$  is the total ultrafine number concentrations measured by the SMPS-CPC,  $N_{UF}^n$  the normalised number concentrations, and  $U$  the wind speed averaged over the measurement time. The denominator is the linear equation for the 10 m distance from the roadside. The numerator (22464) gives the number of particles calculated at the wind speed averaged over the eight measurement days ( $\approx 6$  m/s). Similar computations were performed for the data collected at the 45 and 90 m as well as for the A9 data and the average downwind gradients of the number concentrations could be calculated. The results for both motorways are given in Figure 3.8 including the average number concentration for background air measured upwind. Clearly, the decrease of particle numbers downwind from the motorway can be approximated satisfactorily with exponentially decaying functions. It is estimated that at 10 m from motorway the ultrafine particle numbers are 5 to 8 times higher than upwind. After 75 m numbers have been reduced by a factor of two. Extrapolation of the trendlines indicates that at a downwind distance of 200 m the vehicular contribution has reduced to zero as numbers are of the same order as the upwind (background) level.

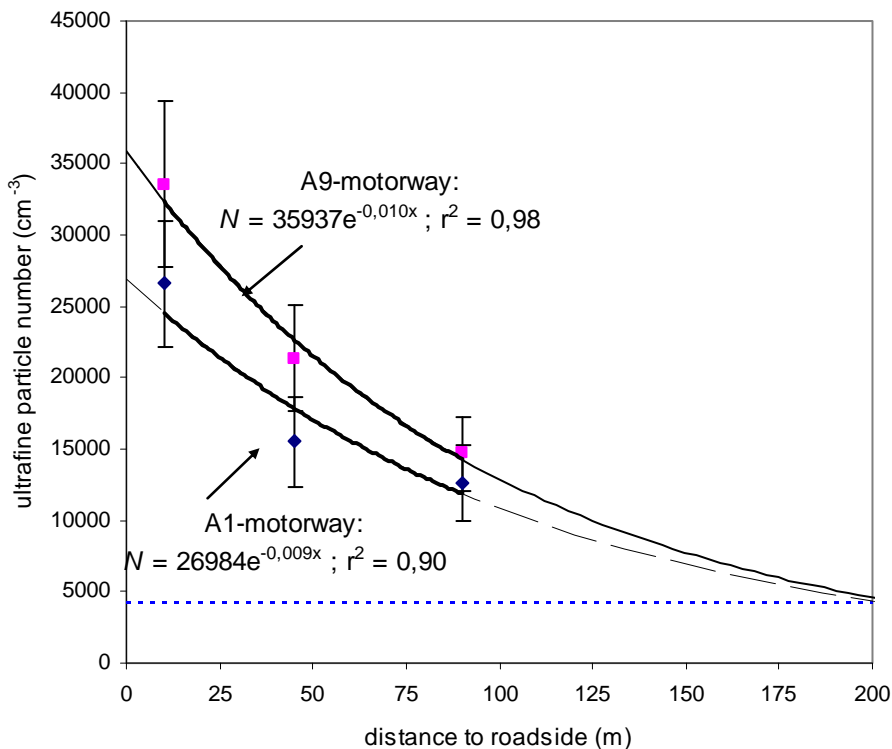


Figure 3.8 *Gradients of the number of ultrafine particles (with standard deviation) along the A1 and A9 motorway (after correcting for the wind speed effect). Also given the average background concentration level and exponential approximations*

### 3.4 Changes in number size distributions at increasing distance from the motorway

The average particle number distributions measured downwind at 10, 45 and 90 m and upwind are shown in Figures 3.9 - 3.12. Figure 3.13 gives the results after subtraction of the upwind levels. These are averages over the normalised data collected at the eight measurement days along both motorways. The horizontal axis represents the particle diameter on a logarithmic scale. The effects of the vehicular emissions on the downwind particle size distributions are apparent. The upwind distributions appear more consistent (having smaller standard deviations). The downwind measurements show a far greater variation as (individual) distributions change quickly between measurements. Obviously, the vehicular sources vary widely in their emission characteristics, this variation having the greatest effect on the measurements closest to the motorway.

Also, the shape of the upwind differs from the ones observed at the downwind locations. Upwind a single mode exists, peaking around 35 nm while the roadside distributions suggest maximum numbers below 13 nm (the lowest size channel of the SMPS). The absolute numbers in the smaller diameter ranges differ largely. For example, at 10 m from the motorway the number of particles with a diameter of 13 nm is more than 18 times higher than in upwind air. Several authors have reported the presence of a mode around 10 nm (e.g., Kittelson, 1998; Zhu et al., 2002; Sturm et al., 2003; Wehner, 2004). The dominance of the freshly-emitted traffic particles with sizes below 50 nm is also found in dynamometer experiments (Baumgard and Johnson, 1996; van Helden, 2000).

At 45 and 90 m this mode is weaker but still present (Figures 3.10 - 3.11): at 90 m the particle number at a diameter of 13 nm is three times the upwind value. It is supposed that upwind measurements here take place in 'aging' air originally containing particles emitted by traffic and industrial sources at considerable distances. Due to the various aerosol processes (dilution, coagulation, condensation, deposition) these particles are absent in the background distribution.

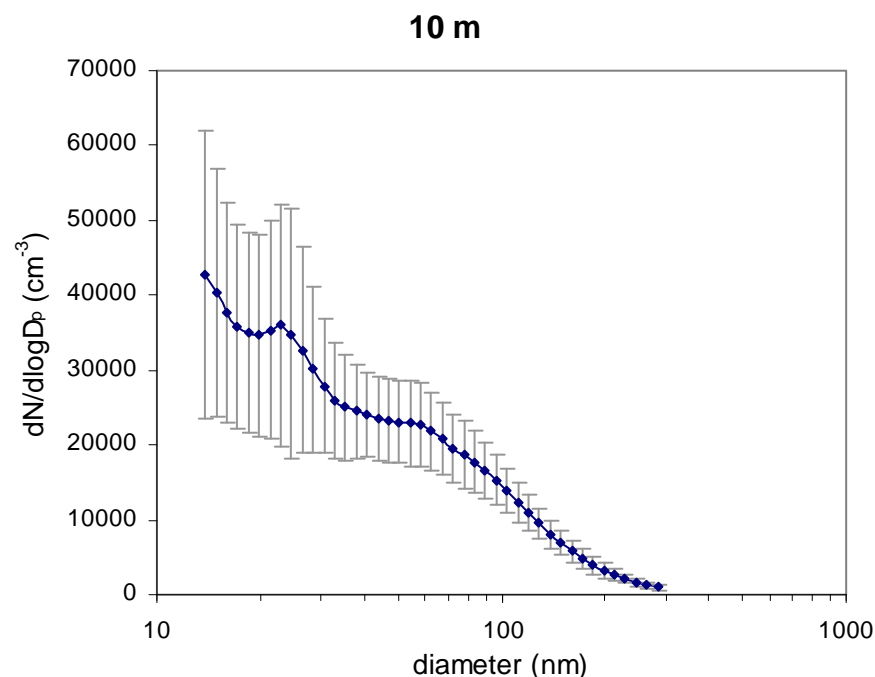


Figure 3.9 *Average particle size distributions for the 8 measurement days (corrected for wind speed dilution effect) at 10 m; measurement range SMPS-CPC: 13-284 nm diameter.*

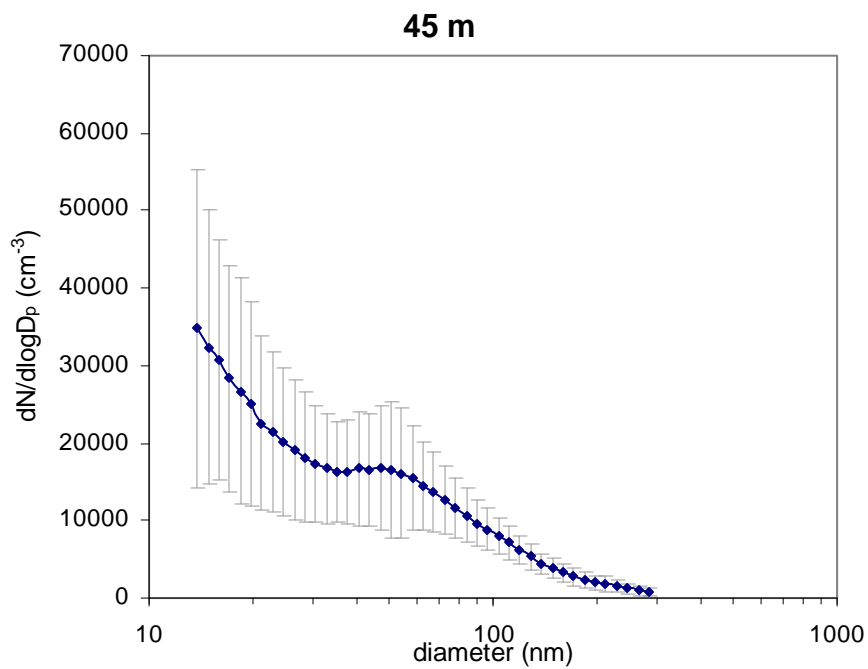


Figure 3.10 *As Figure 3.9 but now at 45 m*

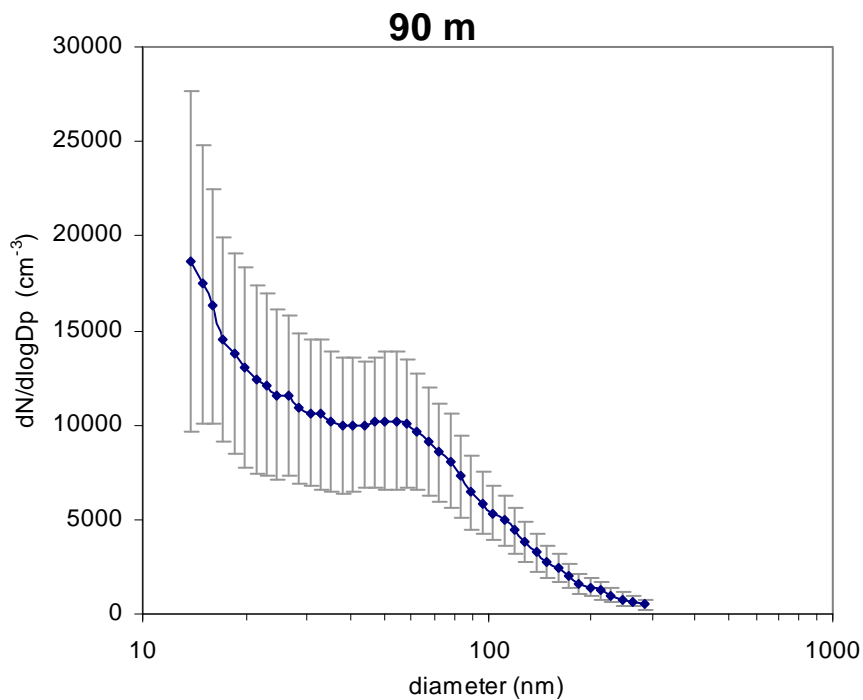


Figure 3.11 *As Figure 3.9 but now at 90 m*

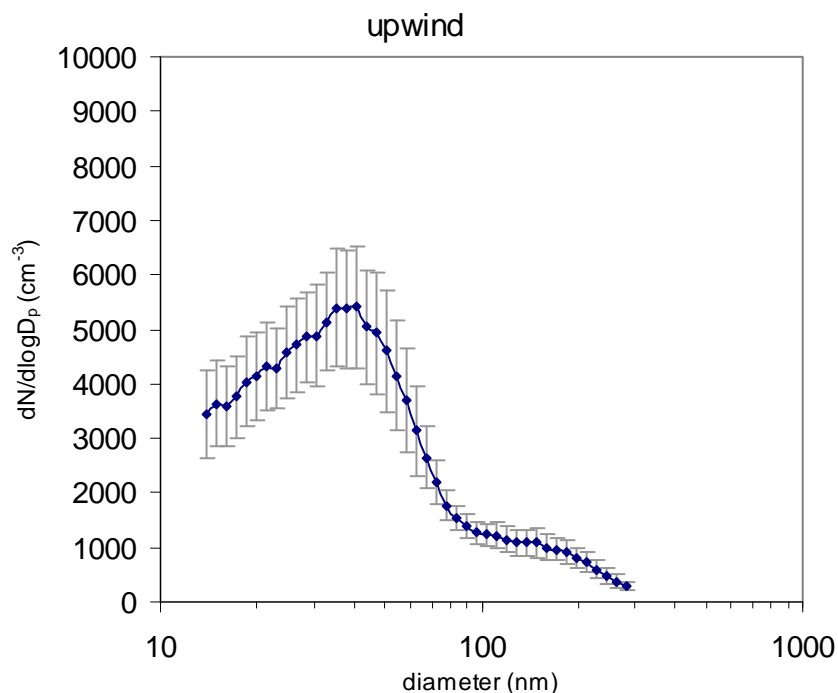


Figure 3.12 As Figure 3.9 but now at the upwind location

At 10 m also a relative maximum around 23 nm is observed which has entirely disappeared at a distance of 45 m. Baumgard and Johnson (1996) described such a mode in dynamometer tests of diesel engines. Figures 3.9 - 3.11 further display a ‘saddle area’ for particles within the size range 40-60 nm. Further downwind this saddle has turned into a more pronounced maximum peaking at sizes around 50 and 70 nm, respectively. Such a phenomenon implies that the rate of decrease in particle number with increasing distance from the road is not equal for the various particle diameters. The changes in the particle size distributions during the wind driven transport is a net result of several processes: production (nucleation of hot gasses in the car’s tailpipe and exhaust pipe), dilution due to local wind turbulence, condensation of vapours on the particles surface as well as the reverse process (evaporation), coagulation (particles colliding to form larger particles), and deposition on the ground. All these processes will affect number concentrations to a various degree, depending on ambient (atmospheric) conditions and depending on particle size (except dilution).

To demonstrate this, the relative decrease in particle number within three particle fractions (<40 nm, 40-80 nm, and >80 nm) during the wind driven transport from 10 to 90 m has been calculated (see Figure 3.14). In the case of the smallest particles (with the largest numbers) it is found that 64% of them has ‘disappeared’ at 90 m. In the next size range (40-80 nm), the particle number decreases less (57%). Dilution is effective irrespective of particle diameter (for the sizes considered here). Hence, the different rates of change should be due to some other process. If coagulation and/or condensation occur, some of the particles become part of the succeeding fraction (40-80 nm), thereby decreasing the particle numbers of the first fraction and increasing those of the second fraction. Hence, the decrease in particle number in the latter fraction will be less than in the former. However, the same figure reveals that the relative loss of particles above 80 nm is again larger. The reasons for this may be that for this size range the condensational growth rate decreases with increasing particle size and that coagulation is most effective under conditions with high particle number, i.e. at smaller sizes. A first-order estimate of the effect of coagulation on the decrease in particle number,  $N$ , can be made as follows:  $\Delta N \approx k_{coagulation} \cdot N^2$ . For a typical (size dependent) coagulation rate constant of  $4 \cdot 10^{-9} \text{ cm}^3 \text{ s}^{-1}$ , this amounts to a decrease of  $3-10 \text{ particles cm}^{-3} \text{ s}^{-1}$  (decreasing strongly as the total particle number

decreases from e.g. 50000 to 25000  $\text{cm}^{-3}$ ). This suggests that coagulation is of minor importance compared to dilution, and probably also compared to condensation. This will be discussed in more detail in the next chapter, by means of rigorous modelling of these processes.

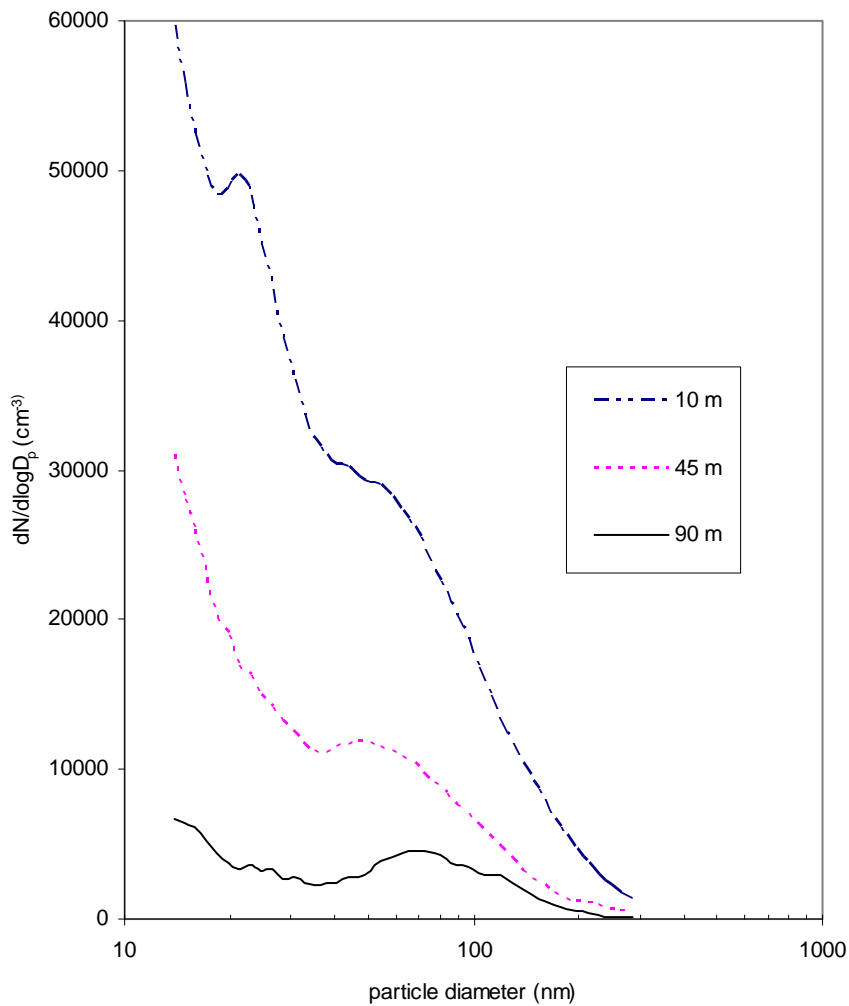


Figure 3.13 *Average size distributions measured at 10, 45 and 90 m with upwind contribution subtracted*

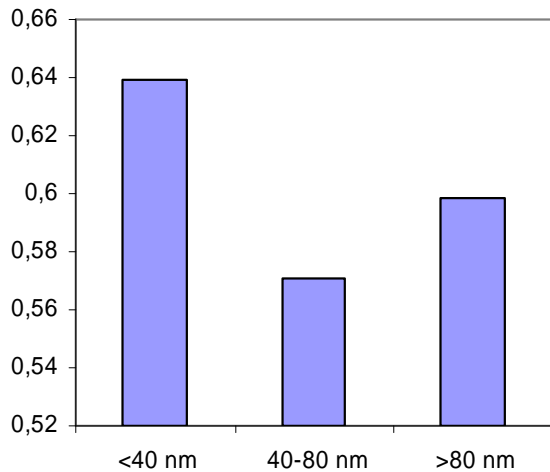


Figure 3.14 *Relative decrease of particle numbers for three size fractions during the wind-driven transport from the 10 m site to the 90 m site*

### 3.5 Modelling aerosol dynamical processes

Two case studies were examined in more detail using the aerosol dynamics model PARGAN (Particle Growth and Nucleation; Verheggen and Mozurkewich, 2006). The average size distributions as measured on the 26<sup>th</sup> of September are given in Figure 3.15, where the distance to the road has been translated into an effective transport time from the motorway to the sampling unit, using an average wind speed of 2.5 m/s.

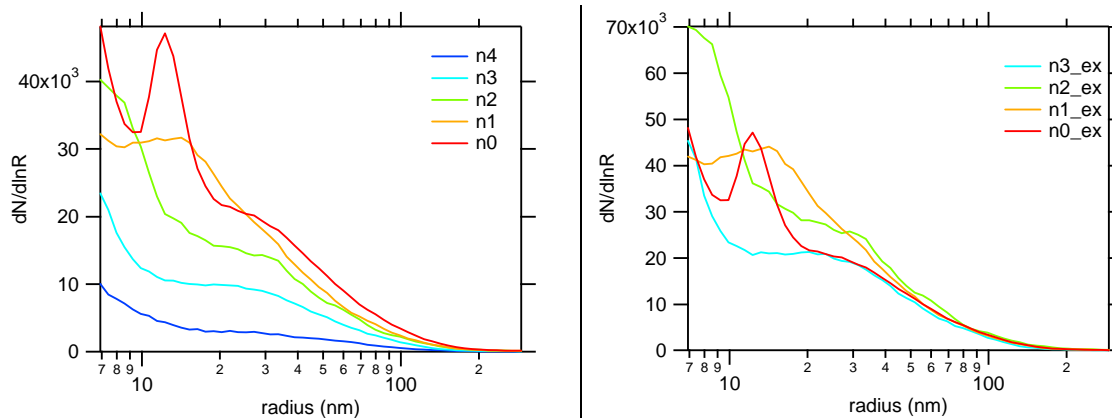


Figure 3.15 *Measured size distributions (particles  $\text{cm}^{-3}$ ) on September 26 (left panel), averaged for each distance to the motorway. The index number refers to the location, where n0 denotes 10 m downwind, n1 the 25 m, n2 the 40 m, and n3 the 80 m, and n4 is upwind of the motorway (background). The right panel gives the same distributions, corrected for dilution using  $\text{NO}_x$  as a tracer. Note that particle radius is used here instead of diameter.*

The graph on the left shows the distributions as they were measured, while the graph on the right provides the distributions, scaled towards the first, least diluted one. This is done by using the  $\text{NO}_x$  ( $=\text{NO}+\text{NO}_2$ ) concentrations as a tracer for dilution, assuming that on these time scales other processes only marginally affect the  $\text{NO}_x$  gradient. If the particles ( $N$ ) are diluted to the same extent as  $\text{NO}_x$ , then we can write (see e.g. Zhang and Wexler, 2004):

$$\frac{N(x_1) - N_{bg}}{N(x_2) - N_{bg}} = \frac{NO_x(x_1) - NO_{x,bg}}{NO_x(x_2) - NO_{x,bg}}$$

Where the index  $x_i$  stands for location  $i$  with respect to the motorway, and  $bg$  stands for background (i.e. upwind of the motorway). This equation can be rewritten and used to correct the size distribution data (at each distance  $x_i$ ) for dilution, using the least diluted stage (10 metres distance,  $n\theta$ ) as a reference ( $x_{ref}$ ):

$$N_{corr}(x_i) = (N(x_i) - N_{bg}) \times \left( \frac{NO_x(x_{ref}) - NO_{x,bg}}{NO_x(x_i) - NO_{x,bg}} \right) + N_{bg}$$

The ‘corrected’ distributions are shown on the right; the background distribution,  $n_d$ , is absent from this figure, since it can not be defined using this correction scheme.

Even though the assumption of equal mixing for all substances sounds very reasonable, the concentrations of the different species were found to decay with slightly different rates, as shown in Figure 3.16 below, where the background value is arbitrarily set at 200 seconds travelling time from the motorway.

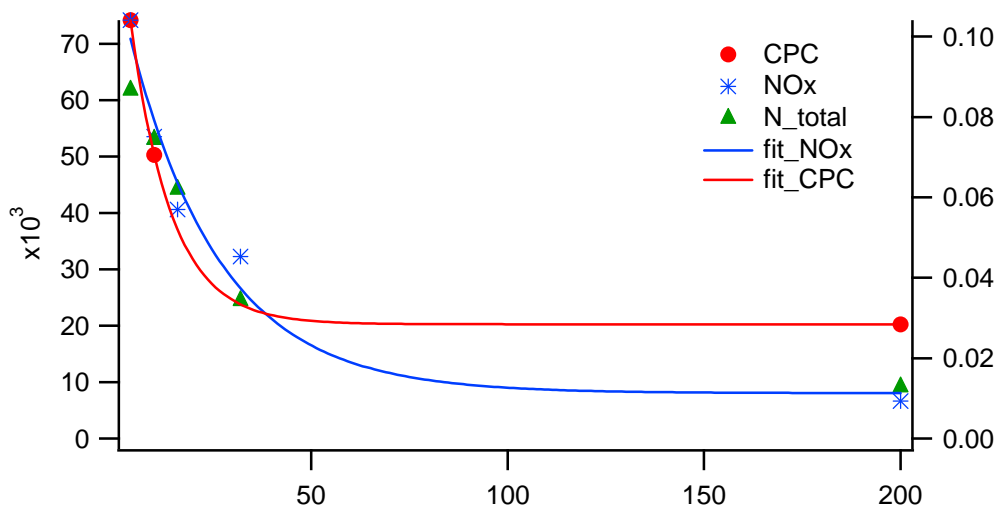


Figure 3.16 *Decay of particle and NO<sub>x</sub> concentrations with increasing travelling time (in seconds) from the motorway. The background values are arbitrarily set at 200 seconds. Particle concentrations (as measured by CPC and the SMPS integral, N<sub>total</sub>) are noted on the left axis (particles/cm<sup>3</sup>) and NO<sub>x</sub> on the right axis (ppm). An exponential decay is fitted to the CPC and NO<sub>x</sub> data.*

An exponential fit to the NO<sub>x</sub> and CPC data (concentration =  $y_0 + A \exp(-Kt)$ ) results in the following parameters for the decay constant,  $K$ :

NO<sub>x</sub> vs t:

$$K = 400 \text{ /h (} y_0 = 0.042 \text{)}$$

(asymptotic background value,  $y_0$ , allowed to vary)

$$K = 150 \text{ /h (} y_0 = 0.0093 \text{)}$$

(asymptotic background value,  $y_0$ , fixed at the measured value of 0.0093)

CPC vs t  
 $K = 350 \text{ /h}$  ( $y_0 = 20267$ )  
(all three points exactly fitted)

With the shortcomings mentioned above in mind, it is immediately obvious that dilution has a very strong effect on the gradient that is measured at different distances from the highway. The remainder changes in the distributions, in as far as they are not due to errors in the correction procedure or to noise/variability in the data, are due to aerosol dynamics: Processes acting on the distribution of particles amongst different sizes. These processes are nucleation, condensation, coagulation, and deposition.

Since the distributions on this day have been measured between 14 and 600 nm diameter, the effect of nucleation of new particles can not be directly observed. Its effect is indirectly observed from growth of small particles into the measured size range. Condensation of semi-volatile gases causes the particles to grow in size. Coagulation refers to the collision of two particles and subsequent formation of one bigger particle; it decreases the total number of particles, while it conserves total volume. Deposition of particles to the ground is a loss process for both aerosol number and volume. These processes (except deposition, which was deemed negligible on these short time scales) were included in an inverse simulation of the measurements, to arrive at estimates of their relative importance.

The inverse modelling procedure PARGAN attempts to fit the measured change in the size distributions by a quantitative description of these processes. The measured distributions act as input parameters to the model. By means of regression analysis, the optimal value for a set of user-defined variables is found. Typically, the particle growth rate is such a variable of interest, since it can not be easily quantified in another way. We also attempted to verify the dilution rate this way. Coagulation rates are theoretically well known, and are included as such in the procedure.

The change in the measured size distribution over each time step is fitted by a theoretical description of these processes (see Verheggen and Mozurkewich for details). As the parameter being fitted, either the change in the regular size distribution function is taken ( $dn/dt$ ) or the change in the cumulative size distribution ( $dN_c/dt$ ), where  $N_c$  denotes the total number of particles above a certain size. Ideally, both should give the same result, but measurement noise/variability usually causes this not to be the case. The particle growth rates that are found by analysing the dilution-corrected distributions (Figure 3.15, right panel) are shown in Figure 3.17. These growth rates denote the change in particle radius over time (nm/h) due to condensation, that provide the best fit between the theory and the measurements of  $dn/dt$  and  $dN_c/dt$ .



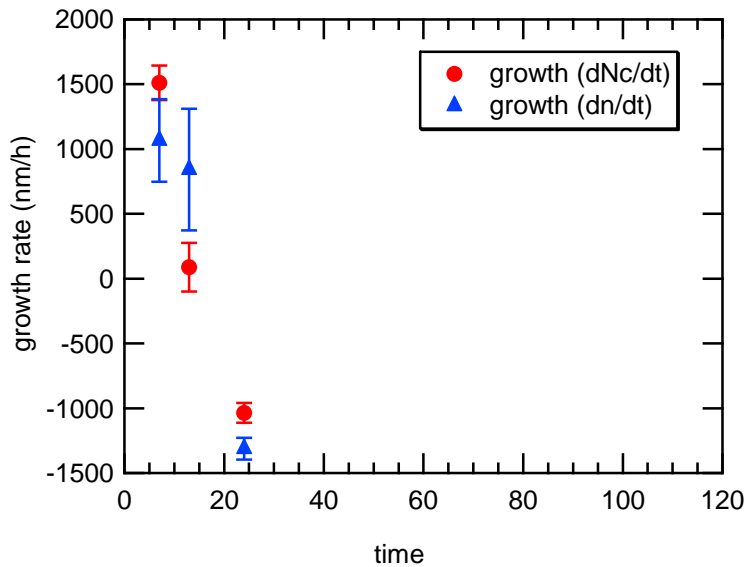


Figure 3.17 *Radius growth rates as found using PARGAN by analysing the change in the dilution-corrected size distributions.*

Figure 3.18 and Figure 3.19 give the contribution of condensation (fitted) and coagulation (prescribed by theory) to the change in the size distributions during the first time interval (from 10 to 25 metres distance). The effect of dilution is already accounted for by means of the procedure described above. The effect of deposition is deemed negligible, in accordance with what has been found at other studies described in the literature. These figures also provide a visual example of what the model procedure PARGAN does: It attempts to find the best match between the sum of contributions (of condensation (=growth) and coagulation in this case) and the measured change (in black squares).

From these analyses it is clear that the effect of coagulation is relatively minor, due to the short time scales. Only a few tens of particles have had time to coagulate with each other in each time step. This is negligible compared to the thousands of particles that are brought into the measured size range and moved across the size spectrum by condensation, for example. Note that the total number of particles ranges from  $60000 \text{ cm}^{-3}$  (10 m) to  $24000 \text{ cm}^{-3}$  (80 m).

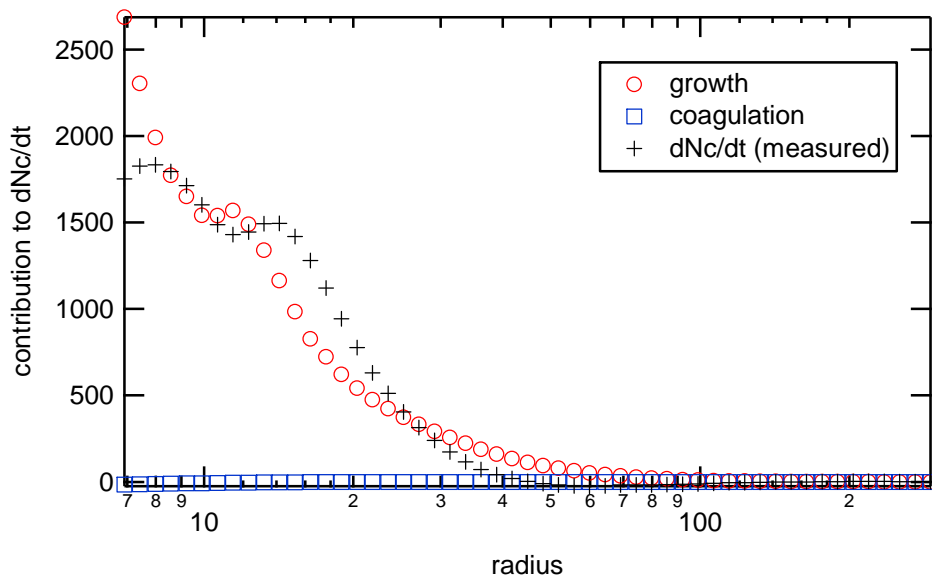


Figure 3.18 *The contribution of different processes to the change in cumulative particle number size distribution (particles  $\text{cm}^{-3}$ ).*

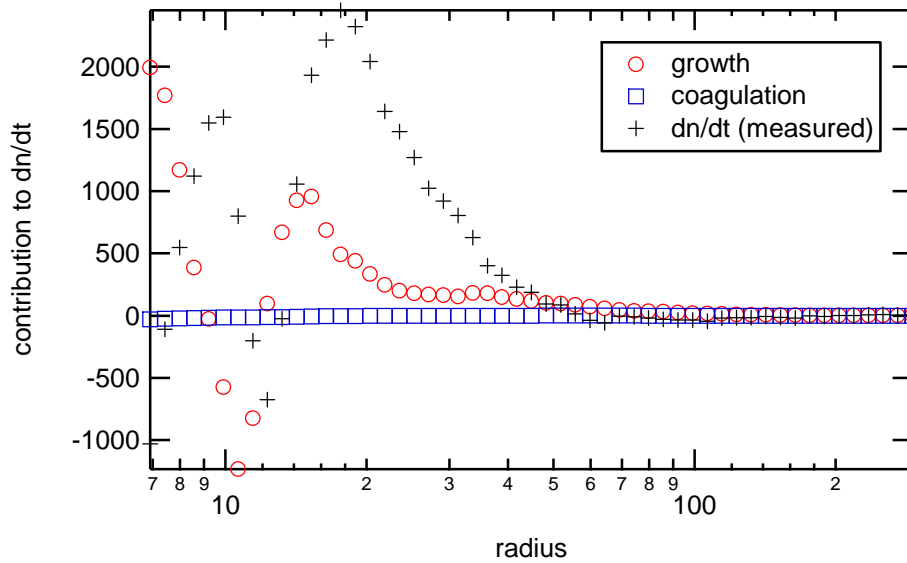


Figure 3.19 *The contribution of different processes to the change in particle number size distribution (particles  $\text{cm}^{-3}$ ).*

Part of the reason for the large negative growth rate (i.e. shrinkage of particles) during the last time interval (from 40 to 80 metres distance) is probably that the correction for dilution was too weak for the last distribution ( $n3\_ex$  in Figure 3.15). But it has also been observed elsewhere (e.g. Zhang and Wexler, 2004) that particles evaporate further away from the highway, when the semi-volatile organics become so diluted that they are no longer supersaturated with respect to their environment, and as a result semi-volatile compounds start to evaporate out of the particles. This could also have contributed to the negative growth rate found here.

The change in the size distributions was also simulated for November 11. Here, the effect of dilution was included in the model, rather than corrected for before model application (as was done for the case of September 26). The results are qualitatively similar: The effect of coagulation on the evolution of the size spectra, as the air is transported away from the motorway, is insignificant. Dilution and condensation are the major influencing factors. If we allow both the particle growth rate and the dilution rate to be optimized by the regression analysis, the following values for the two respective time intervals are calculated:

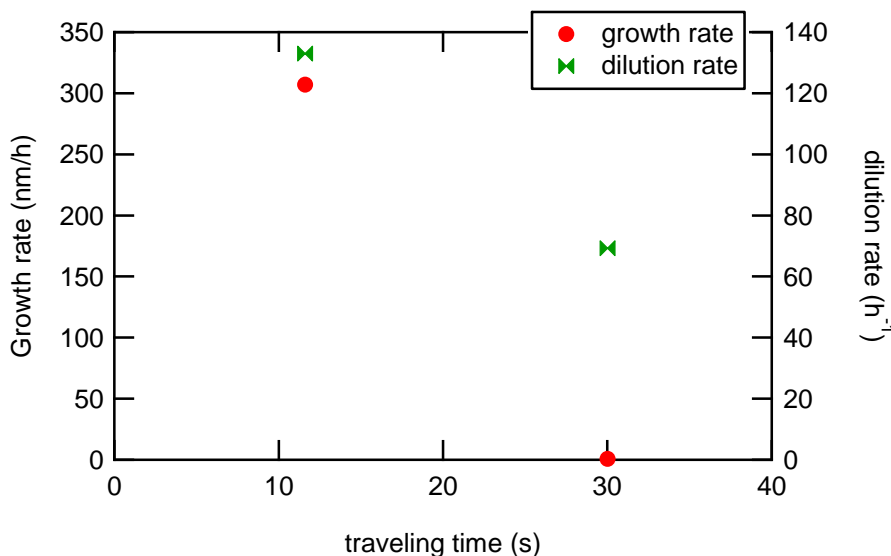


Figure 3.20 *Growth rate and dilution rate constant, as found by regression analysis of the distributions measured on November 11.*

The influence of the different factors on the change in cumulative distributions (number of particles above a certain size) over the first time interval (from 10 to 40 metres distance to the motorway) are shown below.

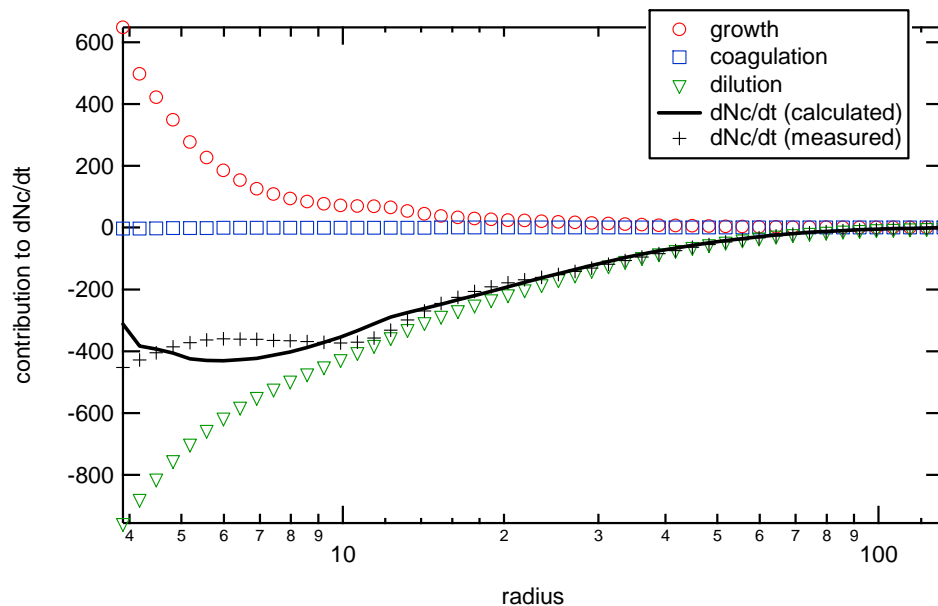


Figure 3.21 *The contribution of different processes to the change in cumulative particle number (particles  $\text{cm}^{-3}$ ). The sum of condensation (=growth), coagulation and dilution gives the calculated change in cumulative number (black squares), which is as close as possible to the measured change (thick black line), by optimizing both the growth rate and the dilution rate (Figure 3.20).*

This shows the negligible effect of coagulation compared to the other processes, and also shows that uncertainty in the dilution rate directly translates in uncertainty of the growth rate that is found by this analysis: they largely have an opposite effect on the change in size spectra, and their values can thus be traded off in the regression analysis of finding the optimal match between the calculated and the measured change in the size distribution.

Close to the motorway, condensation of semi-volatile organics exerts a strong influence on the particles, causing them to grow in size. Further away this influence diminishes, when the organic vapour is no longer super-saturated with respect to the particles in the air. This is the same behaviour as was observed in the dataset for September 26.

### 3.6 Emission factors for ultrafine particle number

One method to quantify vehicular emissions is by measuring the concentrations in the gas stream of motor vehicles that are placed on a dynamometer. Operating according to standardised driving cycles, ‘real-world’ conditions are simulated. However, there is doubt whether such measurements are sufficiently accurate. Emissions from vehicles depend on age and maintenance, factors not always included in these dynamometer testing procedures. Also, the driver’s behaviour is not always captured by the different testing cycles and ‘off-cycle’ driving often leads to higher emissions. Furthermore, the physical and chemical processes occurring directly behind the vehicle’s outlet in the open air may not be representatively reproduced as these depend on the atmospheric conditions (e.g. temperature) and the presence of other pollutants (including particles). To circumvent disadvantages like these, the ‘open-air’ method is applied here (Bloemen en van Putten, 1998; see paragraph 2.3).

The required additional dataset contained 16 sampling periods collected along the A9-motorway during four days. The calculation is done separately for the data collected at the distance of 10 m, and the combined data belonging to 45 and 90 m. Emission factors for CO<sub>t</sub> and NO<sub>xt</sub> have been extracted from two Dutch references: (i) input dataset used in the CARI model (Teeuwisse, 2002), and (ii) study of the effects of traffic conditions on vehicular emissions on Dutch motorways (Gense et al., 2001). Both give data representative for Dutch motorways in the year 2001. Emissions factors, in particular those for LDV, vary with speed. On average (free flow with a propagation speed above 75 km/h) the emission factor (and standard error) per vehicle for CO<sub>t</sub> is 1.82(0.91) g/km for LDV and 1.34(0.09) for HDV; in case of NO<sub>xt</sub> these values are 0.71(0.19) and 7.16(1.34), respectively.

The emission factors for the ultrafine particle numbers are estimated on basis of the linear regression analyses according to Eq.[4]. Background concentrations were subtracted to obtain vehicular contributions. The regression plots are given in Figure 3.22. The scatter in these plots is relatively small. The uncertainty in the result depends on the uncertainty in the emission factors for CO<sub>t</sub> and NO<sub>xt</sub>, and the uncertainty in the regression factors *p* and *q* of Eq.[4]. Table 3.1 gives the resulting factors for both HDV and LDV with corresponding standard error. Clearly, the emission factor turns out to be lower when data from the more distant measurements are used. This can be explained by coagulation leading to a faster decrease of ultrafine particle numbers with distance compared to the gaseous components.

Table 3.1 *Estimated emission factors for ultrafine particle number (in number of particles per km and per vehicle)*

<i>Emission factor (<math>\cdot 10^{15} \text{ km}^{-1} \text{ veh}^{-1}</math>)</i>		
<i>distance to roadside</i>	10 m	45 and 90 m
<i>LDV</i>	0.30 ( $\pm 0.23$ )	0.23 ( $\pm 0.90$ )
<i>HDV</i>	3.1 ( $\pm 1.2$ )	2.1 ( $\pm 0.5$ )

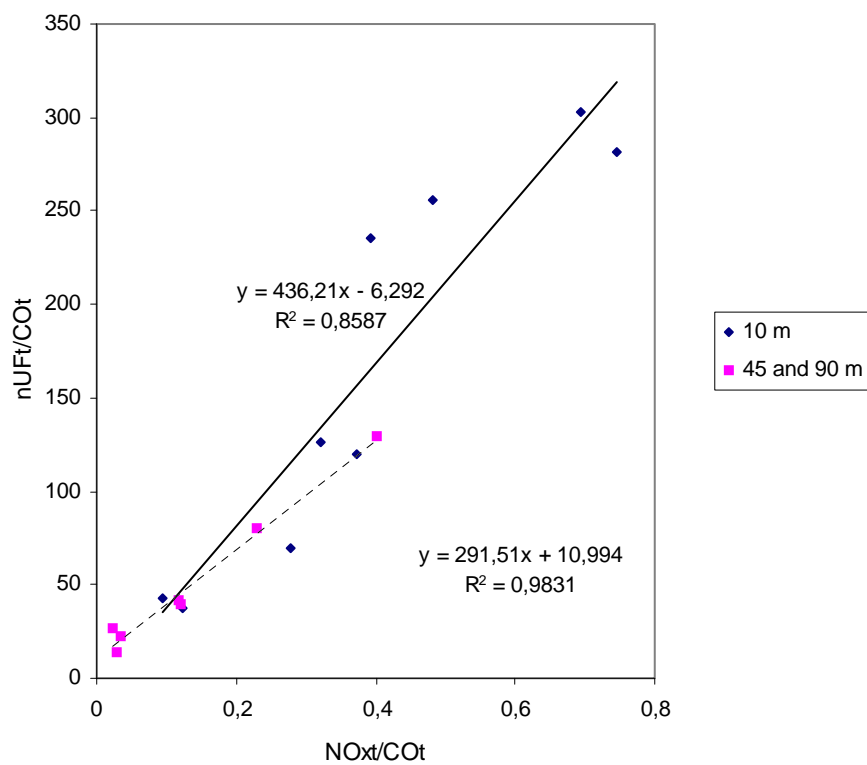


Figure 3.22 *Regression analyses for the A9 data*

## 4. Conclusions

Number concentrations and size distributions of the ultrafine particle fraction were investigated near two motorways in the Netherlands. The measurements took place at increasing distances from the roadside and at one upwind location. The traffic emission on the motorway largely dominates the total number concentrations as well as the size distributions of the ultrafine particles downwind from the motorway (in comparison to their upwind characteristics). Particle numbers measured downwind are affected by wind speed and wind direction, and also depend on the vehicular propagation and density on the motorway. Due to more dilution a negative linear trend in the ultrafine number concentrations is seen when wind speed increases (in the range 3-8 m/s). At a certain distance from the roadside (45 m) lower particle numbers are measured when the angle of the prevailing wind direction with the normal direction (to the motorway) increases. Also, a higher vehicle speed increases the ultrafine numbers present near the motorway which is due to a higher engine load. Heavily congested traffic on the motorway leads to a rise in ultrafine particle numbers near the motorway, which probably originates from the irregular engine load (frequent deceleration and acceleration) and more vehicles per unit length.

In order to study changes in particle number concentrations and size distributions during the transport downwind, times with congested conditions were discarded from the dataset. Measurements took place during periods with different prevailing wind speeds. In order to use these data, corrections for the corresponding varying dilution effect were applied first. It is then found that the decreases of the total ultrafine particle numbers (summed up to 100 nm) with increasing distances to the motorways can accurately be described by an exponentially decaying function. At 10 m downwind from the motorway it is observed that the ultrafine particle concentrations are approximately 5-8 times higher compared to average levels measured upwind. At 200 m the vehicular contribution is of the same order as the background concentration.

The vehicular influence becomes even more apparent in the size distributions measured in downwind air. These reveal that most of the particles are smaller than 50 nm even at 90 m from the roadside. At 10 m distance from the motorway it is found that the number concentration of particles with a diameter of 13 nm is more than 18 times the concentration in background air. Findings like these show that people living, working or travelling within approximately 200 m of a (similar) motorway are exposed to (much) elevated levels of ultrafine particles. A 'nanoparticle mode' or 'nuclei mode' forms when exhaust gases come into contact with outer air (Kittelson, 1998). It is the creation of very fine particles from gases during strong dilution and cooling (nucleation). This process depends on prevailing temperature, humidity and the presence of other particles.

Looking at the size distribution in more detail, a relative maximum in the 10 m distance recording is found at a diameter of 23 nm, which may be attributed to diesel engine emissions. At the same distances the presence of a 'saddle area' between 40 and 60 nm is apparent which becomes more pronounced at 45 and 90 m. This implies that the rate of change of numbers during the wind driven transport starting at 10 m does not take place at the same rate, and that other processes besides dilution affect this change.

The potential influence of other processes was investigated by using the inverse model PARGAN, which simulates the aerosol dynamical processes. The analysis of two case studies shows that besides dilution, condensation and evaporation (presumably of semi-volatile organics) has a strong effect on the change in the measured particle distributions as the air is transported away from the motorway. It first leads to the particles growing in size (in close

proximity to the motorway), while it slows down, and may even revert to evaporation of the semi-volatiles back into the air further downwind (leading to particle shrinkage) and disappearing to the gas-phase. This reversal from growth to evaporation is probably a consequence of the strongly decreasing concentration of semi-volatile vapour in the air as it is being diluted. Coagulation was found to have a negligible effect on the size distributions over the short time scales under investigation.

Emission factors for the ultrafine numbers were calculated by applying a method enabling to distinguish between heavy-duty and light-duty vehicles. The values estimated here, i.e.  $(3 \pm 2.3) \cdot 10^{14}$  particles/km for LDV and  $(3.1 \pm 1.2) \cdot 10^{15}$  particles/km for HDV are similar to data reported elsewhere in spite of differences in experimental setup. For example, Kittelson et al. (2004) published a study focusing on particle emissions on Minnesota highways and estimated emissions of total particle number larger than 3 nm range to be 1.9 to  $9.9 \times 10^{14}$  per km for a gasoline-dominated vehicle fleet. Ketzel et al. (2003) calculate an average fleet emission factor typical for urban conditions in Denmark as  $(2.8 \pm 0.5) \times 10^{14}$  per km (size range: 10-700 nm).

## References

- Baumgard, K.J., Johnson, J.H., 1996. The effect of fuel and engine design on diesel exhaust particle size distribution. Society of Automotive Engineers 960131.
- Bloemen, H.B. Putten, E. van (1998): Mobile emission factor determination through ambient air monitoring - MEDAM project. RIVM report 723301008, the Netherlands.
- Buringh, E., Opperhuizen, A., 2002. On health risk of ambient PM in the Netherlands, RIVM report 650010032, the Netherlands.
- CAFE Working Group on Particulate Matter, 2003. Second Position Paper on Particulate Matter, draft for discussion.
- Dockery, D.W., Pope, C.A., Xu, X., Spengler, J.D., Ware, J.H., Fay, M.E., Ferris, B.G., Speizer, F.E., 1993. An association between air pollution and mortality in six US cities. *New Engl. J. Med.* 329, 1753-1759.
- Donaldson, K., Beswick, P.H., Gilmour, P.S., 1998. Free radical activity associated with the surface of particles: a unifying factor in determining biological activity? *Toxicol. Let.* 88, 293-298.
- Donaldson, K., Stone, V., Clouter, A., Renwick, L., Macnee, W., 2001. Ultrafine particles. *Occup. Environ. Med.* 58, 211-560.
- Ferin, J., Obersorster, G., Penney, D.P., 1992: Pulmonary retention of ultrafine and fine particles in rats. *Am. J. Resp. Cell Mol. Biol.* 6 535-564.
- Harris, S.J., Maricq, M.M., 2001: Signature size distribution for diesel and gasoline engine exhaust particulate matter, *J. Aeros. Sci.* 32, 749-764.
- Helden, R. van: presentation SAE TOPTEC, 4-6 September 2000, Gothenburg, Sweden.
- Hoek G., Brunekreef, B., Goldbohm, R.A., Fischer, P.H., Brandt, P.A. van den, 2002. Association between mortality and indicators of traffic-related air pollution in the Netherlands: a cohort study. *Lancet* 360, 1203-1209.
- Hinds, C.W., 1982. *Aerosol Technology, Properties, Behaviour, and Measurement of Airborne Particles*, J. Wiley and Sons, Inc, 133 pp.
- Hitchins, J., Morawska, L., Wolff, R., Gilbert, D., 2000. Concentrations of submicrometer particles from vehicle emissions near a major road. *Atm. Env.* 34, 51-59.
- Imhof, D., E. Weingartner, C. Ordóñez, R. Gehrig, M. Hill, B. Buchmann, and U. Baltensperger, 2005. Real-world emission factors of fine and ultrafine aerosol particles for different traffic situations in Switzerland. *Environ. Sci. Technol.*, **39**, 8341-8350.
- Jaques, P.A., Kim, C.S., 2000. Measurement of total lung deposition of inhaled ultrafine particles in healthy men and women. *Inhal. Toxicol.* 12, 715-731.
- Kittelson, D.B., 1998. Engines and nanoparticles: a review. *J. Aer. Sci.* 29, 575-588.
- Kittelson, D.B., Watts, W.F., Johnson, J.P. 2004: Nanoparticles on Minnesota highways. *Atm.Env.* 38, 9-19.
- Künzli, N., Kaiser, R., Medina, S., 2000. Public-health impact of outdoor and traffic-related air pollution: a European assessment. *Lancet* 356, 795-801.
- Morawska, L., Bofinger, N.D., Kocis, L., Nwankwoala, A., 1998. Submicrometer and supermicrometer particles from diesel vehicle emissions. *Environ. Sci. Technol.* 32, 3845-3852.



- Morawska, L., Thomas, S., Gilbert, D., Greenaway, C., Rijnders, E., 1999. A study of the horizontal and vertical profile of submicrometer particles in relation to a busy road. *Atm. Env.* 33, 1261-1274.
- Osunsanya, T., Prescott, G., Seaton, A. (2001): Acute respiratory effects of particles: mass or number? *Occup. Environ. Med.* 58, 154-159.
- Peters, A., Wichmann, H.E., Tuch, T., Heinrich, J., Heyder, J., 1997. Respiratory effects are associated with the number of ultrafine particles. *Am. J. Resp. Crit. Care Med.* 155, 1376-1383.
- Pirjola, L., Parviainen, H., Hussein, T., Valli, A., Hämeri, K., Aalto, P., Virtanen, A., Keskinen, T.A., Mäkelä, T., Hillamo, 2004. 'Sniffer' - a novel tool for chasing vehicles and measuring traffic pollutants. *Atm. Env.* 38, 3625-3635.
- Prevot, A.S.H., Kurtenbach, R., Wiesen, P., 2003. Roadside measurements of particulate matter size distribution. *Atm. Env.* 37, 5273-5281.
- Shi, J.P., Khan, A.A, Harrison, R.M., 1999. Measurements of ultrafine particle concentration and size distribution in the urban atmosphere. *Sci.Total Environ.* 235, 51-64.
- Shi, J.P., Evans, D.E., Khan, A.A, Harrison, R.M.. 2001: Experimental investigation if ultra-fine particle size distribution near a busy road. *Atm. Env.* 35, 1193-1202.
- Verheggen and M. Mozurkewich, 2006: An inverse modelling procedure to determine particle growth and nucleation rates from measured aerosol size distributions, *Atmos. Chem. Phys.* 6, 2927-2942.
- Wehner, B., Philippin, S., Wiedensohler, A., Scheer, V., Vogt, R., 2004. Variability of non-volatile fractions of atmospheric aerosol particles with traffic influence. *Atm. Env.* 38, 6081-6090.
- Weijers, E.P., Khlystov, A.Y., Kos, G.P.A., Erisman J.W., 2004. Variability of particulate matter concentrations along roads and motorways determined by a moving measurement unit. *Atm. Env.* 38, 2993-3002.
- Woo., K.S., Chen, D.R., Pui, D.Y.H., McMurry, P.H., 2001. Measurement of Atlanta aerosol size distributions: observations of ultrafine particle events. *Aerosol Science and Technology* 34, 75-87.
- Zhang, K.M., Wexler, A.S., Zhu, Y.F., Hinds, W.C., Sioutas, C., 2004. Evolution of particle number distribution near roadways. Part II: the 'road-to-ambient' process. *Atmos. Environ.* 38, 6655-6665.
- Zhu, Y., Hinds, W.C., Kim, S., Shen, S., Sioutas, C., 2002a. Study of ultrafine particles near a major highway with heavy-duty diesel traffic. *Atm. Env.* 36, 4323-4335.
- Zhu, Y., Hinds, W.C., Kim, S., Shen, S., Sioutas, C., 2002b. Concentration and size distribution of ultrafine particles near a major highway. *J. Air Waste Man. Ass.* 52, 174-185.